Internucleobase-Interaction-Directed Self-Assembly of Nanofibers from Homo- and Heteroditopic 1,ω-Nucleobase Bolaamphiphiles

Toshimi Shimizu,*[,†,‡,§] Rika Iwaura,[‖] Mitsutoshi Masuda,[†,‡,§] Takeshi Hanada,[†,⊥] and Kiyoshi Yase[†,#]

Contribution from the National Institute of Materials and Chemical Research, 1-1 Higashi, Tsukuba, Ibaraki 305-8565, Japan, Japan Chemical Innovation Institute, NIMC, 1-1 Higashi, Tsukuba, Ibaraki 305-8565, Japan, and CREST, Japan Science and Technology Corporation (JST), 1-1 Higashi, Tsukuba, Ibaraki 305-8565, Japan

Received January 23, 2001

Abstract: The complementary 1,ω-thymine, 1,ω-adenine, and 1,ω-(thymine, adenine) bolaamphiphiles, [*N*,*N*′-bis[3-(2,4-dihydroxy-5-methylpyrimidine-1-yl)propionyl]1,*n*-diaminoalkane [**T-*n*-T** (n = 10, 11, 12)], *N*, *N*′-bis[3-(6-aminopurine-9-yl)propionyl]1,*n*-diaminoalkane [**A-*n*-A** (n = 10, 11, 12)], and *N*-[3-(2,4-dihydroxy-5-methylpyrimidine-1-yl)propionyl], *N*′-[3-(6-aminopurine-9-yl)propionyl]1,*n*-diaminoalkane [**T-*n*-A** (n = 10, 11, 12)], respectively] have been synthesized. The spontaneous homo- and heteroassembly of these nucleobase-based bolaamphiphiles has been studied by light microscopy, energy-filtering transmission electron microscopy, FT-IR, and powder X-ray diffraction analyses. The achiral **T-10-T** bolaamphiphile produced in 10% ethanolic/aqueous solutions unprecedented double-helical ropes of 1−2 μm in widths and several hundred micrometers in length, whereas the complementary homologue **A-10-A** gave only microcrystalline solids of 1−10 μm in size. In contrast, an equimolar mixture of **T-10-T** and **A-10-A** yielded supramolecular fibers of 15−30 nm in width. ^{1}H NMR, CD, and UV studies of solution photoreactions of **T-10-T** suggested that under natural light the chiral rope formation is triggered by photodimerization of trace amounts of the thymine moieties in the **T-10-T** assemblies. Complementary hydrogen bond formation between the thymine−adenine heterobase pairs was found to prevent such a photoreaction and resulted in no chiral rope formation. The heteroditopic **T-12-A** bolaamphiphile self-assembled to form supramolecular fibers. Multilamellar organization was proposed for the homo- and heteroassemblies made of **T-*n*-T** and **A-*n*-A**.

Introduction

Molecular organization via the formation of complementary hydrogen bonds has become a powerful strategy for the construction of well-defined nanostructures.[1] Typically studied self-assembly systems in line with this concept include lyotropic mesophases,[2] supramolecular fibers and membranes,[3] two-dimensional (2-D) monolayers,[4] and supramolecular polymers.[5] The most sophisticated system in nature is double-helical DNA structures stabilized by Watson−Crick hydrogen bond base pairing and aryl stacking interactions between adjacent base pairs.[6] However, individual base pairing between nucleic acid components is generally not performed in aqueous solutions without a double-stranded polynucleotide chain.[7] On the other hand, through the formation of three-dimensional (3-D) multiple hydrogen bond networks, we and other research groups have reported the spontaneous homoassembly of well-defined supramolecular fibers,[8,9] microtubes,[10] and crystals[11−13] from symmetrical bola-form compounds. Considering the advantage of both the hydrogen-bonding complementarity and multiplicity,

† National Institute of Materials and Chemical Research.
‡ CREST, Japan Science and Technology Corp. (JST).
§ Present address: Nanoarchitectonics Research Center, National Institute of Advanced Industrial Science and Technology, Tsukuba Central 5, 1-1-1 Higashi, Tsukuba, Ibaraki 305-8565, Japan.
‖ Japan Chemical Innovation Institute.
⊥ Present address: The Institute of Scientific and Industrial Research, Osaka University, 8-1 Mihogaoka, Ibaraki, Osaka 567-0047, Japan.
Present address: Photonics Research Institute, National Institute of Advanced Industrial Science and Technology, Tsukuba Central 5, 1-1-1 Higashi, Tsukuba, Ibaraki 305-8565, Japan.

(1) (a) Lehn, J.-M.; Mascal, M.; Decian, A.; Fischer, J. *J. Chem. Soc., Chem. Commun.* **1990**, 479−481. (b) Whitesides, G. M.; Mathias, J. P.; Seto, C. T. *Science* **1991**, *254*, 1312−1318. (c) Ghadiri, M. R.; Granja, J. R.; Milligan, R. A.; McRee, D. E.; Khazanovich, N. *Nature* **1993**, *366*, 324−327. (d) Menger, F. M.; Lee, S. J. *J. Am. Chem. Soc.* **1994**, *116*, 5987−5988. (e) Zimmerman, S. C.; Zeng, F.; Reichert, D. E. C.; Kolotuchin, S. V. *Science* **1996**, *271*, 1095−1098. (f) Philp, D.; Stoddart, J. F. *Angew. Chem., Int. Ed. Engl.* **1996**, *35*, 1154−1196. (g) Storhoff, J. J.: Mirkin, C. A. *Chem. Rev.* **1999**, *99*, 1849−1862.

(2) (a) Lehn, J.-M. *Makromol. Chem., Macromol. Symp.* **1993**, *69*, 1−17. (b) Kato, T.; Nakano, M.; Moteki, T.; Uryu, T.; Ujiie, S. *Macromolecules* **1995**, *28*, 8875−8876

(3) (a) Gulik-Krzywicki, T.; Fouquey, C.; Lehn, J.-M. *Proc. Natl. Acad. Sci. U.S.A.* **1993**, *90*, 163−167. (b) Kimizuka, N.; Kawasaki, T.; Hirata, K.; Kunitake, T. *J. Am. Chem. Soc.* **1998**, *120*, 4094−4104.

(4) (a) Sasaki, D. Y.; Kurihara, K.; Kunitake, T. *J. Am. Chem. Soc.* **1992**, *114*, 10994−10995. (b) Boland, T.; Ratner, B. D.; *Langmuir* **1994**, *10*, 3845−3852. (c) Shimomura, M.; Nakamura, F.; Ijiro, K.; Taketsuna, H.; Tanaka, M.; Nakamura, H.; Hasebe, K. *J. Am. Chem. Soc.* **1997**, *119*, 2341−2342.

(5) Sijbesma, R. P.; Beijer, F. H.; Brunsveld, L.; Folmer, B. J. B.; Hirschberg, J. H. K. Ky.; Large, R. F. M.; Lowe, J. K. L.; Meijer, E. W. *Science* **1997**, *278*, 1601−1604.

(6) Saenger, W. *Principles of Nucleic Acid Structure*; Springer: Berlin, 1984.

(7) (a) Nowick, J. S.; Chen, J. S. *J. Am. Chem. Soc*., **1992**, *114*, 1107−1108. (b) Rotello, V. M.; Viani, E. A.; Deslongchamps, G.; Murray, B. A.; Rebek, J., Jr. *J. Am. Chem. Soc*., **1993**, *115*, 797−798.

(8) (a) Fuhrhop, J.-H.; Koening, J. M*embranes and Molecular Assemblies: The Synkinetic Approach;* The Royal Society of Chemistry: Cambridge, U.K., 1994; Vol. 5. (b) Frankel, D. A.; O'Brien, D. F. *J. Am. Chem. Soc*. **1994**, *116*, 10057−10069. (c) Svenson, S.; Kirste, B.; Fuhrhop, J.-H. *J. Am. Chem. Soc*. **1994**, *116*, 11969−11975.

10.1021/ja010201i CCC: $20.00
Published on Web 06/02/2001

we have designed and synthesized 1,ω-thymine-, 1,ω-adenine-, and 1,ω-(thymine, adenine)-appended bolaamphiphiles [*N*,*N*′-bis[3-(2,4-dihydroxy-5-methylpyrimidine-1-yl)propionyl]1,*n*-diaminoalkane [**T-*n*-T** (n = 10, 11, 12)], *N*, *N*′-bis[3-(6-aminopurine-9-yl)propionyl]1,*n*-diaminoalkane [**A-*n*-A** (n = 10, 11, 12)], and *N*-[3-(2,4-dihydroxy-5-methylpyrimidine-1-yl)propionyl], *N*′-[3-(6-aminopurine-9-yl)propionyl]1,*n*-diaminoalkane [**T-*n*-A** (n = 10, 11, 12)], respectively] in which thymine or adenine derivative is homoditopically or heteroditopically connected via amide linkage to both ends of a long *n*-alkyl chain. Except for solution studies by Schall and Gokel[14] and uracil−adenine-based self-assembly studies by Yanagawa et al.,[15] there have been no reports of well-resolved hierarchical nano- and mesostructure construction using thymine−thymine homo- or thymine−adenine heterobase interactions. In analogy with a polynucleotide chain of DNA, a linear amide hydrogen bond chain should facilitate the nucleobase stacking and interactions in the absence of the normal sugar phosphate structures. We are also able to freely tune the internucleobase interactions using either purine−purine, purine−pyrimidine, or pyrimidine−pyrimidine base pairing.[16] In this paper, we describe the formation of supramolecular nucleobase fibers through the spontaneous homoassembly of homoditopic **T-10-T** or heteroditopic **T-12-A** bolaamphiphiles or through the heteroassembly of a 1:1 mixture of **T-10-T** and **A-10-A**.

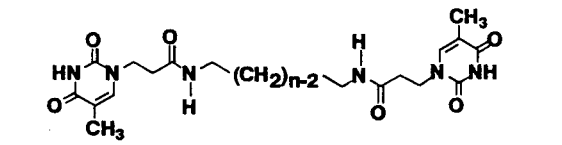

T-n-T (n = 10, 11, and 12)

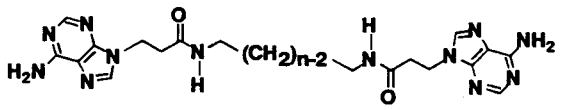

A-n-A (n = 10, 11, and 12)

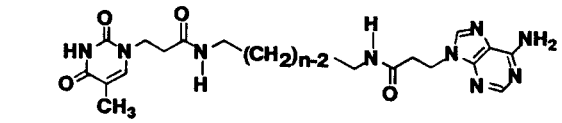

T-n-A (n = 10, 11, and 12)

Results

Light Microscopic Observation of Homo- and Hetero-assemblies. Among the homoditopic 1,ω-nucleobase bolaamphiphiles, the longer derivatives **T-11-T**, **T-12-T**, **A-11-A**, and **A-12-A** proved only sparingly soluble in aqueous solutions ($< \sim 9 \times 10^{-4}$ M at 50 °C), whereas the decamethylene-bridged complementary components **T-10-T** and **A-10-A** showed relatively good solubility ($\sim 1.9 \times 10^{-3}$ M). The heteroditopic bolaamphiphiles **T-*n*-A** (n = 10, 11, 12) displayed solubilization behavior similar to that of homoditopic homologues. Thus, the self-assembly of the homo- and heterobase-pair combination of **T-10-T** and **A-10-A** was investigated in 10% ethanolic/aqueous solutions. The bolaamphiphile **A-10-A** spontaneously self-assembled to form microcrystalline solids of 1−10 μm in size, whereas **T-10-T** produced fibrous assemblies after incubation for a few days. Dark-field light microscopy revealed the formation of a swarm of double-helical ropes from **T-10-T**. Figure 1a clearly displays that two independent chiral ropes of 0.2−1.0 μm in width are helically interwoven each other with the same helical sense. Polarized light microscopy showed that they extend in length to several hundred micrometers (not shown). The helical ropes are very stable in the solution and exhibit no remarkable change in morphology even after one year. The total numbers of left- and right-handed double-helical ropes, calculated for three different pictures, showed an approximately equal preference for each rope (34 and 27 species for the left- and right-handed helical ropes, respectively). In contrast, an equimolar mixture of the complementary **T-10-T** and **A-10-A** components gave an amorphous gel (mp = 202.0−207.0 °C for the dried sample) (not shown).[17] On the other hand, spontaneous homoassembly of the heteroditopic bolaamphiphile **T-12-A** also produced amorphous gel structures in 50% ethanolic-aqueous solutions. The shorter homologue **T-10-A** or **T-11-A** self-assembled to form ordinary microcrystalline solids (not shown).

Transmission Electron Microscopic Observation. To precisely characterize the resultant morphologies and their size dimensions, we observed the individual self-assembled structures using energy-filtering transmission electron microscopy (EF-TEM).[18] Unlike conventional TEM, EF-TEM provides a useful tool for observing low-contrast organic samples without the need for prior staining.[19] The EF-TEM for the helical ropes of **T-10-T** also showed clear images similar to those observed using light microscopy (Figure 1b and c). High-resolution EF-TEM revealed that the helical ropes are composed of very thin ribbons and fibers with widths of more than 14 nm (Figure 1d), with the nanoscale fibers themselves only loosely twisted or helically wound. To date, only a few reports on well-resolved double-helical strands or ribbons formed from *chiral* amphiphiles exist,[8a,20] describing only metastable, intermediate molecular assemblies that slowly convert into higher ordered structures.[20b]

(9) (a) Shimizu, T.; Masuda, M. *J. Am. Chem. Soc.* **1997**, *119*, 2812−2818. (b) Shimizu, T.; Masuda, M.; Kogiso, M.; Asakawa, M. *Kobunshi Ronbunsyu* **1997**, *54*, 815−828. (c) Masuda, M.; Hanada, T.; Okada, Y.; Yase, K.; Shimizu, T. *Macromolecules* **2000**, *33*, 9233−9238.

(10) (a) Shimizu, T.; Kogiso, M.; Masuda, M. *Nature* **1996**, *383*, 487−488. (b) Kogiso, M.; Ohnishi, S.; Yase, K.; Masuda, M.; Shimizu, T. *Langmuir* **1998**, *14*, 4978−4986. (c) Shimizu, T.; Ohnishi, S.; Kogiso, M. *Angew. Chem., Int. Ed. Engl.* **1998**, *37*, 3260−3262.

(11) (a) Shimizu, T.; Kogiso, M.; Masuda, M. *J. Am. Chem. Soc.* **1997**, *119*, 6209−6210. (b) Kogiso, M.; Masuda, M.; Shimizu, T. *Supramol. Chem.* **1998**, *9*, 183−189.

(12) (a) Shimizu, T.; Masuda, M.; Shibakami, M. *Chem. Lett.* **1997**, *12*, 232−234. (b) Masuda, M.; Shimizu, T. *Carbohydr. Res.* **1997**, 302, 139−147.

(13) Coe, S.; Kane, J. J.; Nguyen, T. L.; Toledo, L. M.; Wininger, E.; Fowler, F. W.; Lauher, J. W. *J. Am. Chem. Soc.* **1997**, *119*, 86−93.

(14) Schall, O. F.; Gokel, G. W. *J. Am. Chem. Soc.* **1994**, *116*, 6089−6100.

(15) Itojima, Y.; Ogawa, Y.; Tsuno, K.; Handa, N.; Yanagawa, H. *Biochemistry* **1992**, *31*, 4757−4765.

(16) (a) Ts'o, P. O.; Chan, S. I. *J. Am. Chem. Soc.* **1964**, *86*, 4176−4180. (b) Schwizer, M. P.; Chan, S. I.; Ts'o, P. O. P. *J. Am. Chem. Soc.* **1965**, *87*, 5241−5247.

(17) For 1:1 heteroassemblies formed from **T-11-T**/**A-11-A**, **T-11-T**/**A-12-A**, **T-12-T**/**A-12-A**, and **T-12-T**/**A-11-A** in ethanol, no notable morphologies were observed using light and transmission electron microscopy. For details, see the Supporting Information.

(18) Reimer, L. *Energy-Filtering Transmission Electron Microscopy*; Reimer, L., Ed.; Springer-Verlag: Berlin, 1995.

(19) (a) Nakazawa, I.; Masuda, M.; Okada, Y.; Hanada, T.; Yase, K.; Asai, M.; Shimizu, T. *Langmuir* **1999**, *15*, 4757−4764. (b) Lieser, G.; Schmid, S. C.; Wegner, G. *J. Microsc.* **1996**, *183*, 53−59. (c) Lienemann, C. P.; Mavrocordatos, D.; Perret, D. *Mikrochim. Acta* **1997**, *126*, 123−129.

(20) (a) Fuhrhop, J. H.; Helfrich, W. *Chem. Rev.* **1993**, *93*, 1565−1582. (b)Yanagawa, H.; Ogawa, Y.; Furuta, H.; Tsuno, K. *J. Am. Chem. Soc.* **1989**, *111*, 4567−4570. (c) Sommerdijk, N. A. J. M.; Buynsters, P. J. J. A.; Akdemir, H.; Geurts, D. G.; Pistorius, A. M. A.; Feiters, M. C.; Nolte, R. J. M.; Zwanenburg, B. *Chem. Eur. J.* **1998**, *4*, 127−136.

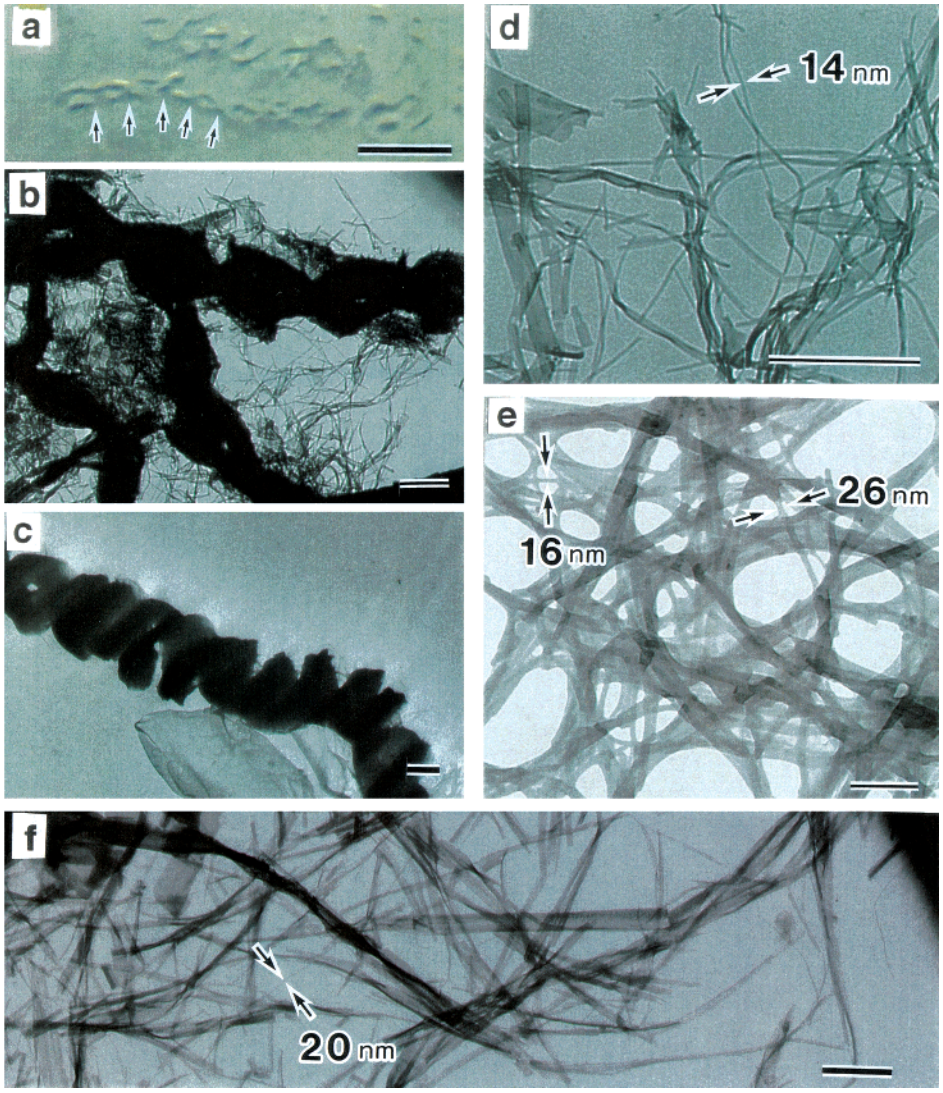

Figure 1. (a) Dark-field light micrograph of double-helical ropes formed from the homoditopic **T-10-T** (at 25 °C in 10% ethanolic/aqueous solutions, bar = 5 μm). The arrows denote representative interwoven portions of the helical ropes. EF-TEM images of (b, c) the double-helical ropes (bar = 1 μm), (d) nanofibers as a constituent of the helical ropes (bar = 1 μm), (e) nanofibers formed from an equimolar mixture of **T-10-T** and **A-10-A** (bar = 200 nm), and (f) nanofibers formed from the heteroditopic **T-12-A** (bar = 1 μm).

To the best of our knowledge, the present finding gives a unique example of stable micrometer-sized double-helical rope formation from an *achiral* component.

An equimolar mixture of the complementary **T-10-T** and **A-10-A** bolaamphiphiles was found to produce nanometer-sized fibers (nanofibers) instead of the chiral double-helical ropes observed for **T-10-T** (Figure 1e). The fibers are of uniform width ranging from 15 to 30 nm, and no significant twisted and helical morphologies could be detected. This implies that the presence of **A-10-A** prevents the helical rope formation of **T-10-T**. The EF-TEM also revealed that the resultant gel structure from the heteroditopic **T-12-A** bolaamphiphile proved to be well-defined nanofibers and nanoribbons of 20−100 nm in width and several hundreds micrometers in length (Figure 1f). Though the base pairing of the heteroassembly (**T-*n*-T** + **A-*n*-A**) should be identical with that of the homoassembly (**T-*n*-A**), the **T-*n*-A** bolaamphiphiles exhibited a chain-length effect[21] that needs a relatively longer oligomethylene spacer for the fiber formation.

Infrared Spectroscopy. Characteristic IR absorption bands of the obtained homo- and heteroassemblies are summarized in Table 1 together with their assignments. Figure 2 displays partial FT-IR spectra of the self-assemblies from the homo- and heteroditopic bolaamphiphiles (n = 10). For the dried helical ropes of **T-10-T**, the amide and imide N−H bands appeared at 3329 and 3160 cm^{-1}, respectively,[22] clearly indicating the formation of hydrogen bonds (Figure 2g). The appearance of the amide I (C═O stretching) bands at 1655−1649 cm^{-1} is also indicative of the formation of an amide hydrogen bond chain within the homo- and heteroassemblies.[23] The frequencies of the CH_2 antisymmetric and symmetric stretching bands are compatible with high trans conformational populations in the oligomethylene spacer.[9,24] For the 1:1 heteroassembly, the amide and imide N−H bands are remarkably shifted from those observed for the single components.[25] In particular, the lower-frequency shift[1a] of the adenine N−H stretching band from 3137

(21) Masuda, M.; Vill, V.; Shimizu, T. *J. Am. Chem. Soc.* **2000**, *122*, 12327−12333.

(22) Kyougoku, Y.; Lord, R. C.; Rich, A. *J. Am. Chem. Soc.* **1967**, *89*, 496−504.

(23) (a) Buchet, R.; Sandorfy, S. *J. Phys. Chem.* **1983**, *87*, 275−280. (b) Graindourze, M.; Smets, J.; Zeegers-Huyskens, T.; Maes, G. *J. Mol. Struct.* **1990**, *222*, 345−364.

(24) Snyder, R. G.; Strauss, H. L. *J. Phys. Chem.* **1982**, *86*, 5145−5150.

(25) For FT-IR spectral change of the equimolar mixture of **T-11-T**/**A-11-A** and **T-12-T**/**A-12-A**, see the Supporting Information.

Table 1. FT-IR Absorption Bands and Their Assignment for the Dried Homo- and Heteroassemblies from **T-10-T**, **A-10-A**, and **T-10-A**

assignment	homoassembly[a]			1:1 heteroassembly[a]
	T-10-T	**A-10-A**	**T-10-A**	**T-10-T/A-10-A**
amide N−H str	3329	3308	3424	3316
			3311	
amine N−H str		3137	∼2750	∼2780
imide N−H str	3160		∼3223	3206[b]
				3108[b]
ring C−H str	3038			
CH_2 antisym str	2928	2930	2932	2928
CH_2 sym str	2855	2851	2851	2855
aromatic C═O str	1694		1687	1695
amide C═O str (amide I)	1651	1655	1643	1649
		1641[c]		
NH_2 scissoring + ring C−H str		1603	1599	1603
amide N−H def (amide II)	1553	1543	1541	1543
CH_2 scissoring def	1470	1489	1474	1478
		1450	1464	1461
CH_2 rocking def	716	731	729	723

[a] Self-assembly was carried out in 10% ethanolic/aqueous solutions. [b] Unidentified shoulder. [c] Hydrogen-bonded NH_2 scissoring plus ring C−H stretching.

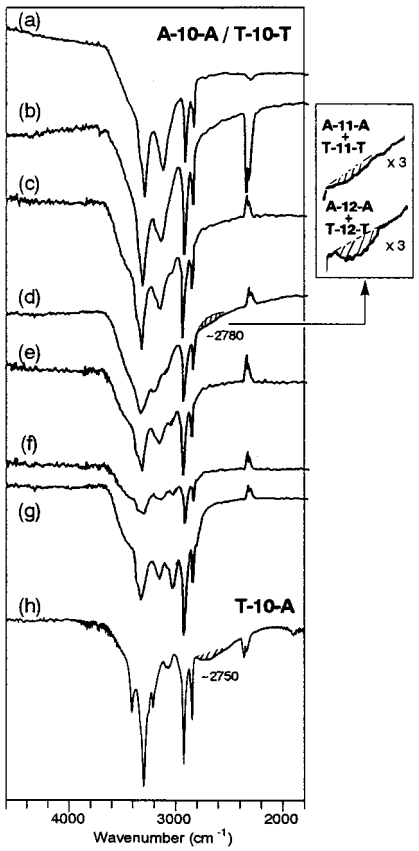

Figure 2. FT-IR spectra (1800−4600 cm^{-1}) of the **T-10-T** homoassemblies, the **A-10-A** homoassemblies, and the heteroassemblies formed from their mixtures. Molar ratio of **T-10-T** to **A-10-A**: (a) 0.0, (b) 0.2, (c) 0.4, (d) 0.5, (e) 0.6, (f) 0.8, and (g) 1.0. Partial FT-IR spectra (∼2780 cm^{-1}) of the equimolar mixture of **T-11-T**/**A-11-A** and **T-12-T**/**A-12-A** are shown as an inset. FT-IR spectra (1800−4600 cm^{-1}) of the **T-10-A** homoassembly is also shown in (h).

to 2780 cm^{-1} (shoulder) and its broadening strongly suggest the formation of complementary 2-D hydrogen bonds between the thymine and adenine moieties (Figure 2a and d). The IR spectral features of the self-assembled heteroditopic bola-amphiphiles **T-*n*-A** (n = 10, 11, 12) are compatible with those of the corresponding heteroassemblies from **T-*n*-T** and **A-*n*-A** (for n = 10, see Figure 2d and h).

The CH_2 scissoring bands also showed distinctive features on moving between the homo- and heteroassemblies (Table 1). The sharp band at 1470 cm^{-1} observed for **T-10-T** indicates the presence of triclinic packing (T//)[24] of the oligomethylene chain within the helical ropes, whereas two separated bands at 1461 and 1478 cm^{-1} observed for the **T-10-T**/**A-10-A** heteroassembly suggest chain packing in an orthorhombic structure (O⊥) within the nanofibers. The dried homo- and heteroassemblies from **T-11-T**, **A-11-A**, **T-12-T**, and **A-12-A** also gave similar FT-IR results (Details are in the Supporting Information).

Powder X-ray Diffraction. Powder X-ray diffraction diagrams of the dried assemblies from **T-10-T**, **A-10-A**, a 1:1 mixture of **T-10-T**/**A-10-A**, and **T-10-A** are shown in Figure 3. The small-angle diffraction pattern of the helical ropes from **T-10-T** shows at least four ordered reflection peaks with a long period of 3.48 nm (Figure 3a). The wide-angle reflection peaks at d = 0.393 and 0.375 nm are characteristic of triclinic packing (T//),[26] which is consistent with FT-IR results. The diffraction diagram of the microcrystalline solids from **A-10-A** can be similarly characterized by the reflection peaks, which suggest a layered structure with a 2.36-nm period and orthorhombic packing (O⊥) (Figure 3b). Once again, the X-ray diagram of the heteroassembly (Figure 3c) is remarkably different from those of its components, with at least two ordered reflection peaks appearing with 2.53- and 1.62-nm-long periods. For this heteroassembly, an orthorhombic packing (O⊥) of the oligomethylene chains supported by FT-IR can also be deduced by three characteristic peaks at d = 0.425, 0.393, and 0.367 nm. Reflection peaks around d = 0.48−0.49 nm, associated with the interchain distance when linked with hydrogen-bonded amide groups,[27] appear for both homoassemblies (Figure 3a and c). On the other hand, the powder X-ray diffraction patterns for the homoassembly from the heteroditopic **T-10-A** bola-amphiphile displayed a single reflection peak attributable to a 1.89-nm-long period as well as well-resolved three peaks (d =

(26) (a) Garti, N.; Sato, K. *Crystallization and Polymorphism of Fats and Fatty Acids*; Marcel Dekker: New York, 1988. (b) Yamada, N.; Okuyama, K.; Serizawa, T.; Kawasaki, M.; Oshima, S. *J. Chem. Soc., Perkin Trans. 2* **1996**, 2707−2714. (c) Parikh, A. N.; Schivley, M. A.; Koo, E.; K.Seshadri; Aurentz, D.; Mueller, K.; Allara, D. L. *J. Am. Chem. Soc.* **1997**, *119*, 3135−3143. (d) Goto, M.; Asada, E. *Bull. Chem. Soc. Jpn.* **1978**, *51*, 2456−2459.

(27) Leiserowitz, L.; Tuval, M. *Acta Crystallogr., Sect. B* **1978**, *34*, 1230−1247.

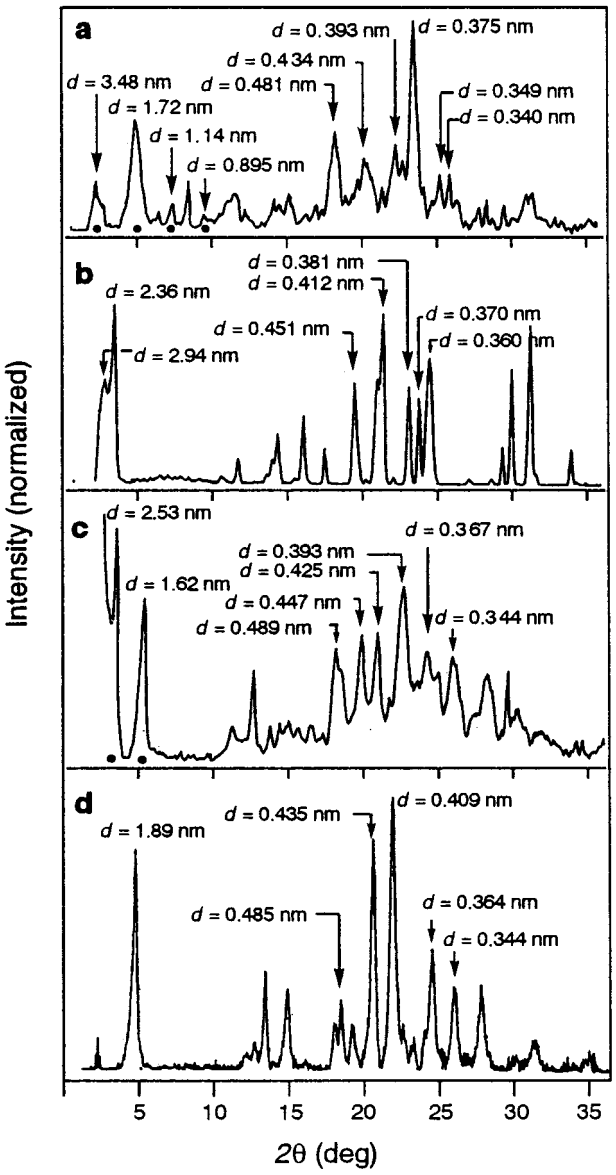

Figure 3. Powder X-ray diffraction diagrams (reflection mode) of (a) the **T-10-T** homoassemblies, (b) the **A-10-A** homoassemblies, (c) the equimolar **T-10-T**/**A-10-A** heteroassemblies, and (d) the **T-10-A** homoassemblies.

0.435, 0.409, and 0.364 nm) based on an orthorhombic oligomethylene packing (O⊥) (Figure 3d). Similar layered structures can also be confirmed for the homo- and hetero-assemblies of the longer bolaamphiphiles **T-11-T**, **A-11-A**, **T-12-T**, and **A-12-A** (Details are in the Supporting Information).

Discussion

A Possible Formation Mechanism of Double-Helical Ropes. The double-helical rope formation from the achiral **T-10-T** bolaamphiphile is incompatible with well-known results showing that enantiomeric compounds should form mirror-imaged assemblies.[8,9,20,28−30] In fact, careful circular dichroism (CD) study demonstrated that the aqueous solutions containing thymine used as a starting material or the final product **T-10-T** have no significant Cotton effect up to the detection limit of the CD apparatus ($\theta < 0.003°$ for absorbance ~1).[31] However, pyrimidine bases are known to reversibly photodimerize and photodissociate by irradiation of higher ($\lambda > 270$ nm) and lower ($\lambda < 270$ nm) wavelength UV light, respectively.[32] It should be noted here that the photodimerization between two thymine derivatives affords four stereoisomers, among which cis-anti- and trans-syn-type isomers are chiral.[33] Under natural light, however, no significant UV spectral changes were observed for the aqueous solution containing **T-10-T** ($c = 9.2 \times 10^{-5}$ M). Photodimerization of the 1,ω-thymine bolaamphiphiles at both ends should afford mixtures such as cyclic dimers, linear trimers, and linear oligomers. Actually, monochromated UV irradiation ($\lambda = 280$ nm) of the same aqueous solutions caused a photoreaction that can be confirmed by the constant decrease in the 271-nm absorbance. After a 50-h irradiation in the presence of acetone (20 wt %) as a sensitizer, we successfully obtained macrocyclic photodimers cyclo**(T-10-T)$_2$** (Figure 4) as a mixture of four isomers. In addition, we also prepared a photodimeric mixture of 1-(2-carboxyethyl)thymine **T-d-T** in a similar manner as that reported elsewhere.[34]

Next we compared ^{1}H NMR spectra of the isolated double-helical ropes with those of the photodimerized derivatives cyclo**(T-10-T)$_2$** and **T-d-T**. The ^{1}H NMR spectra of the distinct photodimers can be characterized by four singlets around $\delta =$ 10.4−10.6 ppm and one singlet at $\delta = 6.5$ ppm (Figure 5b and c). The former signals are assignable to non-hydrogen-bonded imide NH protons of the photodimerized thymine moiety, whereas the latter is assignable to hydrogen-bonded imide NH protons of the photodimer. Figure 5a indicates that one small ($\delta = 8.30$ ppm) and one tiny ($\delta = 6.53$ ppm) singlet newly appear for the dried helical ropes. From the concentration dependence of ^{1}H NMR measurement using a nonaged **T-10-T** sample, the singlet (**m**) at $\delta = 8.30$ ppm can be attributable to hydrogen-bonded imide NH protons of the thymine. Meanwhile, the tiny signal at $\delta = 6.53$ ppm ("Y") appears at identical chemical shift with the non-hydrogen-bonded imide NH protons of the photodimer (Figure 5b and c). These findings strongly suggest that during incubation trace amounts of photodimeric impurities are generated under natural light. The chemical shifts for the imide NH protons of the thymine dimers sensitively reflect their stereoisomeric structures. We should note here that a very tiny signal ("X") at 10.6 ppm of the helical rope corresponds well to the lowest magnetic field signal of the four singlets. Furthermore, that signal is not attributable to a cis-syn (signal q) and cis-anti (signal r) isomer.[34] Therefore, a chiral trans-syn isomer could be a plausible candidate of the trigger substance.[35] The isomer would provide enantiomeric chiral sources in the assemblies and induce the formation of mirror-imaged double-helical ropes. Indeed, the helical rope structures were reproducible by the spiking experiment where the **T-10-T** samples are incubated in the dark in the presence of 5% molar macrocyclic photodimer cyclo**(T-10-T)$_2$**. In contrast, the self-assembly of the **T-10-T** molecules in the dark produced no double-helical ropes.

(28) (a) Tachibana, T.; Kambara, H. *J. Am. Oil. Chem. Soc.* **1965**, *87*, 3015−3016. (b)Nakashima, N.; Asakuma, S.; Kim, J.-M. *Chem. Lett.* **1984**, 1709−1712.

(29) Fuhrhop, J.-H.; Schnieder, P.; Boekema, E.; Helfrich, W. *J. Am. Chem. Soc.* **1988**, *110*, 2861−2867.

(30) Yamada, N.; Sasaki, T.; Murata, H.; Kunitake, T. *Chem. Lett.* **1989**, 205−208.

(31) For high-resolution CD spectra of thymine and **T-10-T**, see the Supporting Information.

(32) Wang, S. Y. *Nature* **1963**, *200*, 879−880.

(33) Wulff, D. L.; Fraenkel, G. *Biochim. Biophys. Acta* **1961**, *51*, 332−339.

(34) Moghaddam, M. J.; Hozumi, S.; Inaki, Y.; Takemoto, K. *J. Polym. Sci. Polym. Chem. Ed.* **1988**, *26*, 3297−3308.

(35) Isolation and identification of the photoreaction products from the double-helical ropes were unsuccessful because of their formation in trace amounts under these experimental conditions.

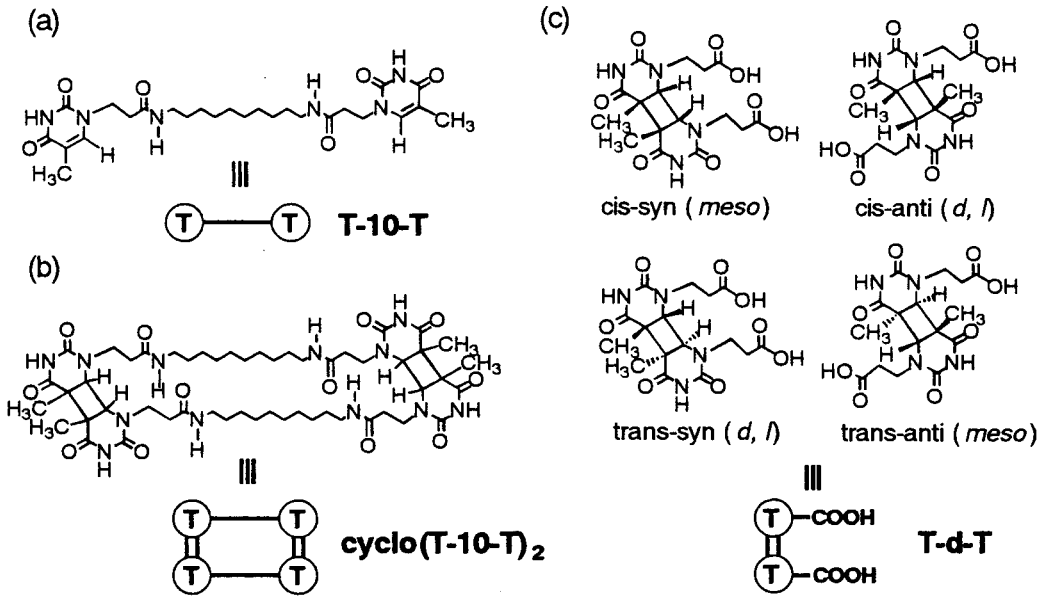

Figure 4. Molecular structures of (a) thymine bolaamphiphile (**T-10-T**), (b) macrocyclic photodimers [cyclo(**T-10-T**)$_2$] of **T-10-T**, and (c) four photodimerized stereoisomers (**T-d-T**) of the thymine carboxyethyl derivative.

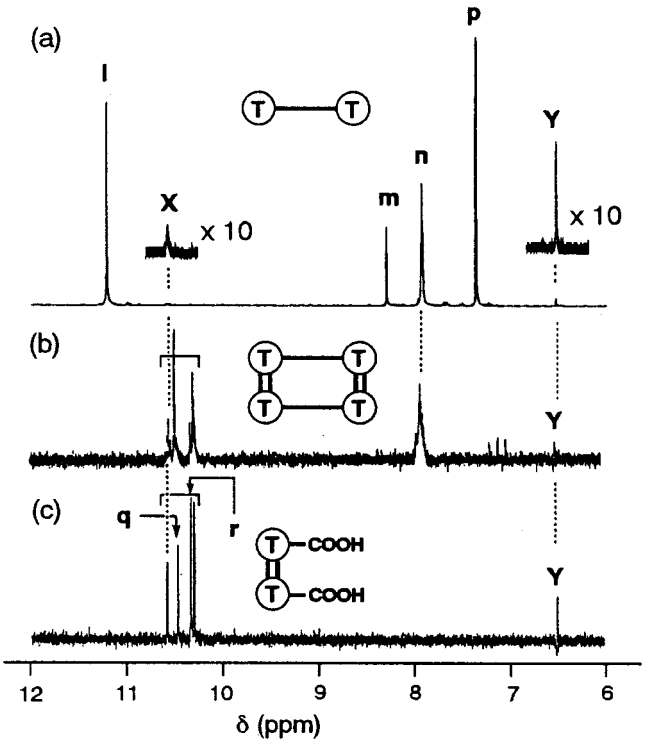

Figure 5. Partial ^{1}H NMR spectra (600 MHz, at 25 °C in DMSO-d_6) of (a) dried double-helical ropes of **T-10-T**, (b) macrocyclic photodimers [cyclo(**T-10-T**)$_2$], and (c) photodimers (**T-d-T**) of the carboxyethyl thymine derivative. Thymine imide N−H, thymine ring C−H, and amide N−H protons of **T-10-T** are denoted by the symbols l, p, and n, respectively. New signals generated by the photoreaction are denoted by the symbols X and Y.

Once the complementary base pairing of the thymine and adenine is formed, such a situation will hinder the thymine moiety from taking an appropriate orientation for the photodimerization. Consequently, the heteroassembly of **T-10-T** and **A-10-A** will result into no helical rope formation. Osmotic and ^{1}H NMR studies indicate that purine−pyrimidine interactions are more favorable than those between pyrimidine bases.[16] This means that the thymine photodimerization is prevented in the presence of the complementary adenine component. Similar inhibition by adenine has already been reported for the photodimerization of thymine-carrying polymers.[36] Thus, the present results may give an interesting example of photochemical mutation within supramolecular assemblies by UV light. In DNA, this has a fatal effect on biological systems.

Table 2. Molar Absorptivity (ϵ) and Absorption Maximums (λ_{max}) of **T-10-T**, **A-10-A**, a 1:1 Mixture of **T-10-T**/**A-10-A**, and Related Compounds in 10% Ethanolic Solutions and Their Hypochromicity

	UV spectral data		reference		
nucleobase derivative	ϵ	λ_{max} (nm)	ϵ_R	λ_{max} (nm)	H (%)
T-10-T	11500	271	8700[b]	271	34[a]
A-10-A	9100	262	13300[c]	262	66[a]
T-10-T/**A-10-A**	13650	262	20600[d]		34[e]
bis(thymine)[f]	17200	270	9700	272	11
purinophane[g]					47.6
purinophane[h]					47.3
pyrimidinopurinophane[i]					30
pyrimidinopurinophane[j]					25

[a] The value of hypochromicity H (%) was evaluated according to the following equation: H (%) = 100(1 − $\epsilon/2\epsilon_R$). [b] The molar absorptivity of thymine. [c] The molar absorptivity of adenine. [d] Summation of the molar absorptivity of **T-10-T** and **A-10-A**. [e] The values of hypochromicity H(%) were evaluated according to the following equation: H (%) = 100(1 − ϵ/ϵ_R). [f] 1,1′-(1,3-Propanediyl)bis[thymine].[37] [g] 1,3-Dithia[3,3](6,9)(9′,6′)purinophane in water.[36] [h] 1,3-Dithia[3,3](6,9)(9′,6′)purinophane in ethanol.[38] [i] In water.[39] [j] In ethanol.[39]

Base Stacking in Homo- and Heteroassemblies. Internucleobase stacking and complementary hydrogen bond formation play an important role in stabilizing the double-helix formation of polynucleotide chains in DNA. To confirm the base stacking interaction in the homo- and heteroassemblies from **T-10-T** and **A-10-A**, we examined their UV spectra in diluted aqueous solutions ($c = 7 \times 10^{-5}$ M). The resulting hypochromism (decrease in UV absorption intensity) was compared with that of related compounds such as bis(thymine)s,[37] -(purinophane)s,[38] and -(pyrimidinopurinophane)s.[39] The UV absorption data of **T-10-T**, **A-10-A**, a 1:1 mixture of **T-10-T**/**A-10-A** complex, and related compounds are summarized in

(36) Kita, Y.; Inaki, Y.; Takemoto, K. *J. Polym. Sci., Polym. Chem. Ed.* **1980**, *18*, 427−439.
(37) Itahara, T. *Bull. Chem. Soc. Jpn.* **1997**, *70*, 2239−2247.

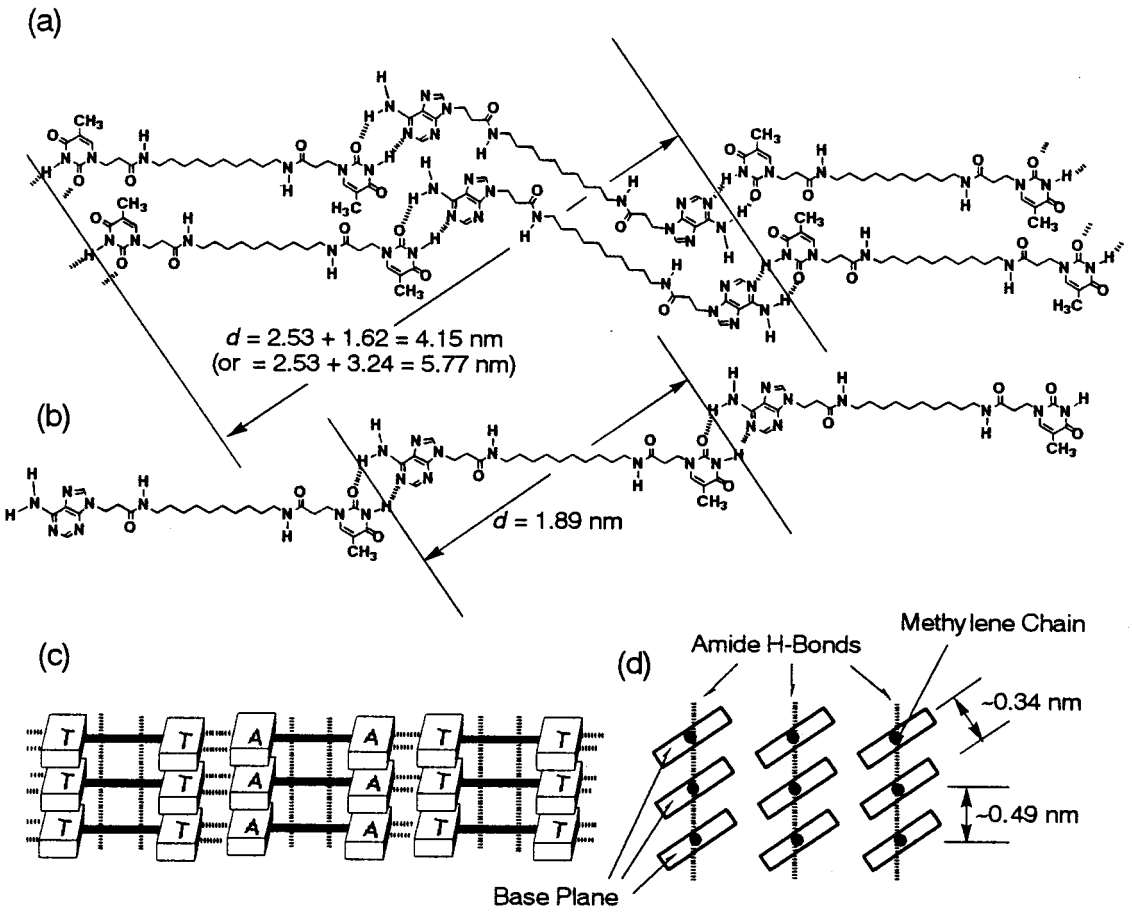

Figure 6. A possible molecular packing and hydrogen bond scheme for (a) the heteroassembly formed from an equimolar mixture of **T-10-T** and **A-10-A** and (b) the homoassembly from **T-10-A**. (a, b) Top view of a layered structure composed of linear polymolecular arrays ("reversed" Hoogsteen base pair configuration is employed here for the thymine−adenine heteroassociation). (c) Front view showing 2-D complementary and 1-D amide hydrogen bond network. (d) Side view of the polymolecular arrays. In (d), the one-dimensional amide hydrogen bond chain contributes to the stabilization of the base stacking and the formation of complementary hydrogen bonds.

Table 2. The hypochromicity values *H* (%) were calculated by a comparison of the absorption intensity with that of a monomeric reference. The *H* value of **T-10-T** was evaluated to be 34%, which is, to the best our knowledge, the largest hypochromicity value reported for thymine-teriminated bola-form compounds such as 1,1′-(α,ω-alkanediyl)bis(thymine)s.[37] The 1,ω-adenine bolaamphiphile **A-10-A** also indicated a much larger *H* value than those so far reported.[38,39] In general, the stacking interaction between pyrimidine bases is considerably smaller than that between purine bases.[16] Therefore, the obtained *H* value of **T-10-T** strongly supports the effective stacking of the pyrimidine bases in the solution. This situation is presumably due to the fixation and stabilization of the bases through the formation of the amide hydrogen bond chain.

Molecular Packing. The X-ray diffraction of the **T-10-T** homoassembly displayed typical reflection peaks (d = 0.340 and 0.349 nm, in Figure 3a) indicative of the formation of vertical base stacking.[6] In addition, its small-angle region suggests that the helical ropes consist of multiple monolayers with a period of 3.48 nm. From the CPK molecular modeling, a fully extended molecular length of **T-10-T** was estimated to be 3.33 nm. If **T-10-T** takes an extended conformation, the molecules should be arranged parallel with respect to the normal to the layer plane. Similarly, the IR and X-ray diffraction studies of the heteroassemblies from **T-10-T** and **A-10-A** indicate the formation of stable layered structures. Considering the two long periods of 2.53 and 1.62 nm (Figure 3c), we could depict lamellar organization in which the molecules should be arranged with tilting to the normal to the layer plane (Figure 6a). Furthermore, the molecules should form linear polymolecular chains through 2-D complementary hydrogen bonds (Figure 6c). The 0.489-nm methylene chain distance supported by X-ray diffraction necessitates tilting of the base plane to achieve the 0.34-nm distance favored for internucleobase stacking (Figure 6d). The above features well resemble the layered 3-D organization of related 1-glucosamide bolaamphiphiles.[9a,12]

X-ray diffraction data indicated the 1.89-nm-long period for the homoassembly of the heteroditopic **T-10-A** bolaamphiphile (Figure 6b), which supports a molecular packing similar to that of the heteroassembly from **T-10-T** and **A-10-A**. Complementary hydrogen bond formation between the heteroditopic molecular ends can also be supported by the FT-IR measurement. In addition, the formation of a linear amide hydrogen bond chain should direct and stabilize the supramolecular nucleobase fiber formation. It is of great interest that the heteroditopic **T-12-A** bolaamphiphile prefers the high aspect ratio structures rather than the microcrystalline solids. This chain-length dependence on the self-assembled morphologies is consistent with that observed for the fiber formation from valylvaline-based bolaamphiphiles.[21,40] In the case of shorter **T-*n*-A** derivatives, they will need relatively stronger internucleobase interactions in order

(38) Seyama, F.; Akahori, K.; Sakata, Y.; Misumi, S.; Aida, M.; Nagata, C. *J. Am. Chem. Soc.*, **1988**, *110*, 2192−2201.
(39) Doyama, K.; Higashii, T.; Seyama, F.; Sakata, Y. Misumi, S. *Bull. Chem. Soc. Jpn.* **1988**, *61*, 3619−3627.

to compensate weak van der Waals forces between the alkyl chains. As a result, strong interlayer interaction between the monolayers might have resulted in 3-D crystalline solids. Thus, the self-assembled morphologies, such as solids, fibers, and double-helical ropes, are found to be strongly dependent on the force strength of the internucleobase interaction. We should note here that four arrangements of the base pairs including Watson−Crick[41] and Hoogsteen types[42] are possible for the configuration of the adenine−thymine base pairs. At present we have, however, no definite evidence for the lateral or vertical arrangement of the individual polymolecular chains.

In summary, spontaneous homoassembly of the 1,ω-thymine bolaamphiphile **T-10-T** produced unprecedented double-helical ropes. The formation may be triggered by trace amounts of photodimerization products within the assemblies. Spontaneous heteroassembly of the complementary 1,ω-thymine and -adenine components and homoassembly of the heteroditopic homologues yielded stable nanofibers instead of the helical ropes. Internucleobase interaction between the resultant monolayers dominated a variety of self-assembled morphologies. The linear amide hydrogen bond chain, like a polynucleotide chain within DNA, was found to stabilize the base stacking and their complementary double hydrogen bonds by fixing them in the internal hydrophobic environment.

Experimental Section

Materials and General Methods. The nucleobases thymine (>98%) and adenine (>99%) were purchased from Merck and were used as received. 1-(2-Carboxyethyl)thymine and 9-(2-carboxyethyl)adenine were synthesized according to a previously described method.[43] Other chemicals were commercially available high-purity grades and were used without further purification. The structures of intermediates and the final products were confirmed by FT-IR, NMR spectroscopy, and elemental analysis. ^{1}H NMR spectra were recorded on a JEOL 600 spectrometer using tetramethylsilane as an internal standard. For the FT-IR measurement, a Jasco FT-IR-620 (resolution 4 cm^{-1}) was used. The UV absorption spectra were recorded at 25 °C on a Hitachi U-3300 spectrometer. CD measurement was performed using a Jasco J-725 spectrometer (sensitivity 0.005°, cell length 5 and 10 mm, temperature 25−70 °C).

Synthesis of 1,ω-Nucleobase-Appended Bolaamphiphiles. The homoditopic 1,ω-thymine bolaamphiphiles **T-*n*-T** (n = 10, 11, 12) were prepared via the coupling of pentachlorophenyl ester of 1-(2-carboxyethyl)thymine with the corresponding long-chain diamines. Similarly, the 1,ω-adenine bolaamphiphiles **A-*n*-A** (n = 10, 11, 12) were synthesized via the coupling of *p*-nitrophenyl ester of 6-trifluoroacetylated 9-(2-carboxyethyl)adenine with the corresponding diamines. On the other hand, the 1,ω-(thymine,amine) bolaamphiphiles **T-*n*-NH$_2$** (n = 10, 11, 12) were prepared via the coupling of pentachlorophenyl ester of 1-(2-carboxyethyl)thymine with an excess amount of corresponding long-chain diamines (10 equiv). Consequently, the heteroditopic **T-*n*-A** bolaamphiphiles (n = 10, 11, 12) were obtainable by the coupling of **T-*n*-NH$_2$** with *p*-nitrophenyl ester of 6-trifluoroacetylated 9-(2-carboxyethyl)adenine. All the final products were then purified by silica gel column chromatography (Yamazen medium-pressure column chromatography system YFLC-6004-FC-GR) to yield white solids. A typical synthetic procedure and related analytical data are as follows.

***N,N′*-Bis[3-(2,4-dihydroxy-5-methylpyrimidine-1-yl)propionyl]-1,10-diaminodecane (T-10-T).** Into a solution of 1-(2-carboxyethyl)-thymine (0.5 g, 2.6 mmol) in DMF (10 mL), pentachlorophenyl trichloroacetate (1.2 g, 2.9 mmol) and triethylamine (0.4 mL) were added. The reaction mixture was stirred at room temperature for 20 h. The resulting mixture was then evaporated in vacuo to give a solid, which was thoroughly washed with cold water. Recrystallization of the raw product from a 1:1 mixture of chloroform and methanol (v/v) gave pentachlorophenyl 3-(2, 4-dihydroxy-5-methylpyrimidine-1-yl)-propionate as a colorless needle crystal (0.4 g, yield 36%). This activated ester (0.3 g, 0.7 mmol) and 1,10-diaminodecane (0.06 g, 0.35 mmol) were then dissolved in DMF (20 mL), and the mixture was stirred at room temperature overnight. The reaction mixture was then evaporated in vacuo to give a solid, which was thoroughly washed with acetone. Purification by silica gel column chromatography (eluent: chloroform/methanol = 2/1, v/v) gave **T-10-T** as a white powder (0.09 g, 50%): mp 210.0−212.5 °C; TLC (silica gel, 1:1 $CHCl_3$/MeOH) R_f = 0.8; ^{1}H NMR (600 MHz, DMSO-d_6, 25 °C) δ 1.20−1.35 (m, 16H, $-CH_2-$), 1.71 (s, 6H, CH_3-5), 2.41 (t, J = 6.6 Hz, 4H, $-CH_2CH_2$CONH-), 3.00 (dt, J = 6.6, 6.6 and 7.2 Hz, 4H, $-$CONHCH_2-), 3.81 (t, J = 6.6 Hz, 4H, $-CH_2CH_2$CONH−), 7.37 (s, 2H, H-6), 7.92 (t, J = 5.4 Hz, 2H, −CONH−), 11.2 (s, 2H, NH-3). Anal. Calcd for $C_{26}H_{40}N_6O_6$: C, 58.63; H, 7.57; N, 15.78. Found: C, 58.77; H, 7.82; N, 15.89.

***N,N′*-Bis[3-(6-aminopurine-9-yl)propionyl]1,10-diaminodecane (A-10-A).** Into a solution of 9-(2-carboxyethyl)adenine (0.4 g, 1.9 mmol) and *p*-nitrophenol (0.3 g, 2.2 mmol) in pyridine (20 mL), *p*-nitrophenyl trifluoroacetate (2.0 g, 8.5 mmol) was added with stirring. The reaction mixture was then stirred at 50 °C for 2 h and then evaporated in vacuo. Solid residues obtained were dissolved in a small amount of chloroform and reprecipitated by addition of diethyl ether. Further reprecipitation from a 1:1 mixture of chloroform and diethyl ether gave *p*-nitrophenyl 3-(6-trifluoroacetoamidopurine-9-yl)propionate as a white powder (0.6 g, yield 75%). Into a solution of this material (0.5 g, 1.25 mmol) in DMF (20 mL), 1, 10-diaminododecane (0.1 g, 0.58 mmol) and imidazole (0.1 g, 1.47 mmol) were added. The mixture was stirred at room temperature for 3 days. The resultant mixture was then evaporated in vacuo to give a raw product, which was thoroughly washed with diethyl ether. Purification by silica gel column chromatography (eluent: $CHCl_3$/MeOH = 9/1−4/1, v/v, gradient) afforded *N, N′*-bis-[3-(6-trifluoroacetoamidopurine-9-yl)propionyl]1,10-diaminodecane (0.1 g, 40%). Deprotection of trifluroacetyl group was carried out by stirring this material in an queous methanolic solution (H_2O/MeOH = 2/5, v/v, 20 mL) of potassium carbonate (7 wt %) overnight. Evaporation of the solvent gave a solid residue which was thoroughly washed with water. Reprecipitation from a 1:1 mixture of ethanol and water (v/v) afforded **A-10-A** as a white powder (0.07 g, 93%): mp 220.1−221.5 °C; TLC (silica gel, 1:1 $CHCl_3$/methanol) R_f = 0.5; ^{1}H NMR (600 MHz, DMSO-d_6, 25 °C) δ 1.17−1.30 (m, 16H, $-CH_2-$), 2.65 (t, J = 6.6 Hz, 4H, $-CH_2CH_2$CONH−), 2.97 (dt, J = 6.0, 6.0, and 7.2 Hz, 4H, −CONHCH_2-), 4.33 (t, J = 6.6 Hz, 4H, $-CH_2CH_2$CONH−), 7.21 (s, 4H, NH_2-6), 7.88 (t, J = 5.4 Hz, 2H, −CONH−), 7.98 (s, 2H, H-8), 8.13 (s, 2H, H-2). Anal. Calcd for $C_{26}H_{38}N_{12}O_2$: C, 57.61; H, 6.96; N, 30.52. Found: C, 57.55; H, 7.07; N, 30.49.

***N*-[3-(2,4-Dihydroxy-5-methylpyrimidine-1-yl)propionyl], *N′*-[3-(6-aminopurine-9-yl)propionyl]1,10-diaminodecane (T-10-A).** The thymine carboxyethyl derivative, pentachlorophenyl 3-(2, 4-dihydroxy-5-methylpyrimidine-1-yl)propionate (0.3 g, 0.7 mmol), and 1, 10-diaminodecane (1.20 g, 7.0 mmol) were then dissolved in DMF (20 mL), and the mixture was stirred at room temperature overnight. The reaction mixture was then evaporated in vacuo to give a solid, which was thoroughly washed with acetone. Purification by silica gel column chromatography (eluent: chloroform/methanol = 2/1, v/v) gave **T-10-NH$_2$** as a white powder (0.09 g, 50%). Into a solution of *p*-nitrophenyl 3-(6-trifluoroacetoamidopurine-9-yl)propionate (0.5 g, 1.25 mmol) in DMF (20 mL), **T-10-NH$_2$** (0.1 g, 0.58 mmol) and imidazole (0.1 g, 1.47 mmol) were added. The mixture was stirred at room temperature for 3 days. The resultant mixture was then evaporated in vacuo to give a raw product, which was thoroughly washed with diethyl ether. Purification by silica gel column chromatography (eluent: $CHCl_3$/MeOH = 9/1∼4/1, v/v, gradient) afforded *N*-[3-(2,4-dihydroxy-5-methylpyrimidine-1-yl)propionyl]-*N′*-[3-(6-aminopurine-9-yl)-propionyl]1,*n*-diaminodecane (0.1 g, 40%): mp 206.0−206.7 °C; TLC (silica gel, 1:1 $CHCl_3$/MeOH) R_f = 0.6; ^{1}H NMR (600 MHz, DMSO-d_6, 25 °C) δ 1.20−1.32 (m, 16H, $-CH_2-$), 1.71 (s, 3H, Thy−CH_3-5),

(40) (a) Kogiso, M,; Hanada, T.; Yase, K.; Shimizu, T. *Chem. Commun*. **1998**, 1791−1792. (b) Kogiso, M.; Okada, Y.; Hanada, T.; Yase, K.; Shimizu, T. *Biochim. Biophys. Acta* **2000**, *1475*, 346−352.

(41) Seeman, N. C.; Rosenberg, J. M.; Suddath, F. L.; Kim, J. J. P.; Rich, A. *J. Mol. Biol.* **1976**, *104*, 109−144.

(42) Hoogsteen, K. *Acta Crystallogr.* **1963**, *16*, 907−916.

(43) Kondo, K.; Sato, T.; Takemoto, K. *Chem. Lett.* **1973**, 967−968.

2.41 (t, J = 6.6 Hz, 2H, Thy-$(CH_2)_2$CONHCH_2CH_2−), 2.65 (t, J = 6.6 Hz, 2H, Ade-$(CH_2)_2$CONHCH_2CH_2−), 2.98 (m, 4H, −CONHCH_2−), 3.81 (t, J = 6.6 Hz, 2H, Thy-CH_2CH_2CONH−), 4.33 (t, J = 6.6 Hz, 2H, Ade-CH_2CH_2CONH−), 7.16 (s, 2H, Ade-NH_2-6), 7.34 (s, 1H, Thy-H-6), 7.89−7.93 (m, 2H, Thy-$(CH_2)_2$−CO*NH*−, Ade-$(CH_2)_2$-CO*NH*−), 7.98 (s, 1H, Ade-H-8), 8.13 (s, 1H, Ade-H-2), 11.2 (s, 1H, Thy-NH-3). Anal. Calcd for $C_{26}H_{39}N_9O_4$: C, 57.65; H, 7.26; N, 22.27. Found: C, 57.89; H, 7.56; N, 22.12.

Spontaneous Homo- and Heteroassembly. Unless otherwise noted, self-assembly experiments were carried out in either 10% ethanolic deionized aqueous solutions for **T-10-T**, **A-10-A**, and **T-10-A** or in ethanol for **T-*n*-T**, **A-*n*-A**, and **T-*n*-A** (n = 11, 12). Ethanol was spectroscopic grade from Wako Chemicals. For the homo- and heteroself-assemblies of **T-10-T**, **A-10-A**, and **T-10-A**, the aqueous solutions (∼5 × 10^{-4} M) were prepared by sonication of a weighed bolaamphiphile sample or their equimolar mixtures at 30 °C (Branson ultrasonicator model 1200, 47 kHz, 60 W). Each solution was allowed to stand at room temperature for 2−3 days. Self-assembled molecular objects in the solutions were then subjected to light microscopy. Preliminary differential scanning calorimetry (DSC) and polarized light microscopic study showed that no thermotropic mesophases were obtained for the dried 1:1 mixtures of **T-*n*-T** and **A-*n*-A** (n = 10, 11, 12).[44]

Light Microscopy and Energy-Filtering Transmission Electron Microscopy. Light microscopic measurement was carried out in a way similar to those described in detail elsewhere.[9a] Unstained specimens for electron microscopy were prepared by placing a 3-μL drop of the supernatant of the dispersion on an amorphous carbon supporting film mounted on a standard TEM grid. The drop was blotted off with filter paper. The dried specimens were examined by electron spectroscopic imaging using an electron microscope (Carl Zeiss EM902) operated at 80 keV with a Castain-Henry-type electron energy filter at room temperature. Zero-loss bright-field images were recorded on an imaging plate (Fuji Photo Film Co., Ltd. FDL 5000) with 20-eV energy windows at 3000−250000× and digitally enlarged.

Powder X-ray Diffraction. Dried samples of the homo- and heteroassemblies were prepared by the careful isolation of the fibers and ropes and their subsequent drying in vacuo. All powder spectra were taken by the reflection or the transmission method with a Rigaku RAD-C powder diffractometer (40 kV and 35 mA) and Rigaku Rotaflex generator RU-200 (40 kV and 150 mA), respectively. The Cu Kα beam was obtained via a graphite monochromator (reflection mode) or a nickel filter (transmission mode). The spectra (reflection method) were measured at room temperature between 1° and 36° in the $2\theta/\theta$-scan mode with steps of 0.01° in 2θ and 0.6-s measurement time per step. The diffraction pattern (transmission method) was recorded with an imaging plate (Fuji Film Ltd., CR ST-VA) in a flat camera.

Photoreaction of 1,ω-Thymine Bolaamphiphiles. Photoreactions of **T-10-T** in 10% ethanolic-aqueous solutions (c = 9.2 ×10^{-5}−4.7 × 10^{-4} M) were carried out in a 10-mm quartz cell at room temperature. The solutions containing acetone (5−20 wt %) as a sensitizer were irradiated with a monochromated high-pressure mercury lamp (λ = 280 nm). The photodimerization was monitored by UV absorbance at 271 nm. Exposure of more than 100 h showed complete disappearance of the 271-nm absorption band. The production of an isomeric mixture of macrocyclic photodimeric derivatives was confirmed by ^{1}H NMR and FAB-MASS (m/z = 1064 $[M + 2Na]^+$). Photodimers of 1-(2-carboxyethyl)thymine were also prepared in a manner similar to that described by Inaki et al.[34]

Acknowledgment. We thank Prof. Y. Inaki of Osaka University for helpful discussions and Dr. T. Takakuwa of Jasco Corp. for CD measurements.

This paper is dedicated to Naresh Dalal on the occasion of his 60th birthday.

Supporting Information Available: Additional experimental data (analytical data, FT-IR spectra, XRD diagrams, and tables showing spectral peak positions) for the homo- and heteroassemblies from the longer **T-11-T**, **A-11-A**, **T-12-T**, and **A-12-A** bolaamphiphiles, which are not discussed above; Light micrographs of the **T-10-T** or **A-10-A** homoassembly; CD spectra of thymine and **T-10-T** bolaamphiphile (PDF). This material is available free of charge via the Internet at http://pubs.acs.org. See any current masthead page for ordering information and Web access instructions.

JA010201I

(44) Paleos, C. M.; Michas, J. *Liq. Cryst*, **1992**, *11*, 773−778.